DESY 95-072, hep-ex/9505003
April 1995

ISSN 0418-9833

A Study of the Fragmentation of Quarks in e^-p Collisions at HERA

H1 Collaboration

Abstract:

Deep inelastic scattering (DIS) events, selected from 1993 data taken by the H1 experiment at HERA, are studied in the Breit frame of reference. The fragmentation function of the quark is compared with those of e^+e^- data. It is shown that certain aspects of the quarks emerging from within the proton in e^-p interactions are essentially the same as those of quarks pair-created from the vacuum in e^+e^- annihilation. The measured area, peak position and width of the fragmentation function show that the kinematic evolution variable, equivalent to the e^+e^- squared centre of mass energy, is in the Breit frame the invariant square of the four-momentum transfer. We comment on the extent to which we have evidence for coherence effects in parton showers.

S. Aid[13], V. Andreev[24], B. Andrieu[28], R.-D. Appuhn[11], M. Arpagaus[36], A. Babaev[26], J. Baehr[35], J. Bán[17], Y. Ban[27], P. Baranov[24], E. Barrelet[29], R. Barschke[11], W. Bartel[11], M. Barth[4], U. Bassler[29], H.P. Beck[37], H.-J. Behrend[11], A. Belousov[24], Ch. Berger[1], G. Bernardi[29], R. Bernet[36], G. Bertrand-Coremans[4], M. Besançon[9], R. Beyer[11], P. Biddulph[22], P. Bispham[22], J.C. Bizot[27], V. Blobel[13], K. Borras[8], F. Botterweck[4], V. Boudry[7], A. Braemer[14], F. Brasse[11], W. Braunschweig[1], V. Brisson[27], D. Bruncko[17], C. Brune[15], R.Buchholz[11], L. Büngener[13], J. Bürger[11], F.W. Büsser[13], A. Buniatian[11,38], S. Burke[18], M. Burton[22], G. Buschhorn[26], A.J. Campbell[11], T. Carli[26], F. Charles[11], M. Charlet[11], D. Clarke[5], A.B. Clegg[18], B. Clerbaux[4], M. Colombo[8], J.G. Contreras[8], C. Cormack[19], J.A. Coughlan[5], A. Courau[27], Ch. Coutures[9], G. Cozzika[9], L. Criegee[11], D.G. Cussans[5], J. Cvach[30], S. Dagoret[29], J.B. Dainton[19], W.D. Dau[16], K. Daum[34], M. David[9], B. Delcourt[27], L. Del Buono[29], A. De Roeck[11], E.A. De Wolf[4], P. Di Nezza[32], C. Dollfus[37], J.D. Dowell[3], H.B. Dreis[2], A. Droutskoi[23], J. Duboc[29], D. Düllmann[13], O. Dünger[13], H. Duhm[12], J. Ebert[34], T.R. Ebert[19], G. Eckerlin[11], V. Efremenko[23], S. Egli[37], H. Ehrlichmann[35], S. Eichenberger[37], R. Eichler[36], F. Eisele[14], E. Eisenhandler[20], R.J. Ellison[22], E. Elsen[11], M. Erdmann[14], W. Erdmann[36], E. Evrard[4], L. Favart[4], A. Fedotov[23], D. Feeken[13], R. Felst[11], J. Feltesse[9], J. Ferencei[15], F. Ferrarotto[32], K. Flamm[11], M. Fleischer[26], M. Flieser[26], G. Flügge[2], A. Fomenko[24], B. Fominykh[23], M. Forbush[7], J. Formánek[31], J.M. Foster[22], G. Franke[11], E. Fretwurst[12], E. Gabathuler[19], K. Gabathuler[33], K. Gamerdinger[26], J. Garvey[3], J. Gayler[11], M. Gebauer[8], A. Gellrich[11], H. Genzel[1], R. Gerhards[11], U. Goerlach[11], L. Goerlich[6], N. Gogitidze[24], M. Goldberg[29], D. Goldner[8], B. Gonzalez-Pineiro[29], I. Gorelov[23], P. Goritchev[23], C. Grab[36], H. Grässler[2], R. Grässler[2], T. Greenshaw[19], G. Grindhammer[26], A. Gruber[26], C. Gruber[16], J. Haack[35], D. Haidt[11], L. Hajduk[6], O. Hamon[29], M. Hampel[1], E.M. Hanlon[18], M. Hapke[11], W.J. Haynes[5], J. Heatherington[20], G. Heinzelmann[13], R.C.W. Henderson[18], H. Henschel[35], I. Herynek[30], M.F. Hess[26], W. Hildesheim[11], P. Hill[5], K.H. Hiller[35], C.D. Hilton[22], J. Hladký[30], K.C. Hoeger[22], M. Höppner[8], R. Horisberger[33], V.L. Hudgson[3], Ph. Huet[4], M. Hütte[8], H. Hufnagel[14], M. Ibbotson[22], H. Itterbeck[1], M.-A. Jabiol[9], A. Jacholkowska[27], C. Jacobsson[21], M. Jaffre[27], J. Janoth[15], T. Jansen[11], L. Jönsson[21], D.P. Johnson[4], L. Johnson[18], H. Jung[29], P.I.P. Kalmus[20], D. Kant[20], R. Kaschowitz[2], P. Kasselmann[12], U. Kathage[16], J. Katzy[14], H.H. Kaufmann[35], S. Kazarian[11], I.R. Kenyon[3], S. Kermiche[25], C. Keuker[1], C. Kiesling[26], M. Klein[35], C. Kleinwort[13], G. Knies[11], W. Ko[7], T. Köhler[1], J.H. Köhne[26], H. Kolanoski[8], F. Kole[7], S.D. Kolya[22], V. Korbel[11], M. Korn[8], P. Kostka[35], S.K. Kotelnikov[24], T. Krämerkämper[8], M.W. Krasny[6,29], H. Krehbiel[11], D. Krücker[2], U. Krüger[11], U. Krüner-Marquis[11], J.P. Kubenka[26], H. Küster[2], M. Kuhlen[26], T. Kurča[17], J. Kurzhöfer[8], B. Kuznik[34], D. Lacour[29], F. Lamarche[28], R. Lander[7], M.P.J. Landon[20], W. Lange[35], P. Lanius[26], J.-F. Laporte[9], A. Lebedev[24], C. Leverenz[11], S. Levonian[24], Ch. Ley[2], A. Lindner[8], G. Lindström[12], J. Link[7], F. Linsel[11], J. Lipinski[13], B. List[11], G. Lobo[27], P. Loch[27], H. Lohmander[21], J. Lomas[22], G.C. Lopez[20], V. Lubimov[23], D. Lüke[8,11], N. Magnussen[34], E. Malinovski[24], S. Mani[7], R. Maraček[17], P. Marage[4], J. Marks[25], R. Marshall[22], J. Martens[34], R. Martin[11], H.-U. Martyn[1], J. Martyniak[6], S. Masson[2], T. Mavroidis[20], S.J. Maxfield[19], S.J. McMahon[19], A. Mehta[22], K. Meier[15], D. Mercer[22], T. Merz[11], C.A. Meyer[37], H. Meyer[34], J. Meyer[11], A. Migliori[28], S. Mikocki[6], D. Milstead[19], F. Moreau[28], J.V. Morris[5], E. Mroczko[6], G. Müller[11], K. Müller[11], P. Murín[17], V. Nagovizin[23], R. Nahnhauer[35], B. Naroska[13], Th. Naumann[35], P.R. Newman[3], D. Newton[18], D. Neyret[29], H.K. Nguyen[29], T.C. Nicholls[3], F. Niebergall[13], C. Niebuhr[11], Ch. Niedzballa[1], R. Nisius[1], G. Nowak[6], G.W. Noyes[5], M. Nyberg-Werther[21], M. Oakden[19], H. Oberlack[26], U. Obrock[8], J.E. Olsson[11], D. Ozerov[23], E. Panaro[11], A. Panitch[4], C. Pascaud[27], G.D. Patel[19], E. Peppel[35], E. Perez[9], J.P. Phillips[22], Ch. Pichler[12], A. Pieuchot[25], D. Pitzl[36], G. Pope[7], S. Prell[11], R. Prosi[11], K. Rabbertz[1], G. Rädel[11], F. Raupach[1], P. Reimer[30], S. Reinshagen[11], P. Ribarics[26], H.Rick[8], V. Riech[12], J. Riedlberger[36], S. Riess[13], M. Rietz[2],

E. Rizvi[20], S.M. Robertson[3], P. Robmann[37], H.E. Roloff[35], R. Roosen[4], K. Rosenbauer[1]
A. Rostovtsev[23], F. Rouse[7], C. Royon[9], K. Rüter[26], S. Rusakov[24], K. Rybicki[6], R. Rylko[20],
N. Sahlmann[2], E. Sanchez[26], D.P.C. Sankey[5], P. Schacht[26], S. Schiek[11], P. Schleper[14], W. von Schlippe[20],
C. Schmidt[11], D. Schmidt[34], G. Schmidt[13], A. Schöning[11], V. Schröder[11], E. Schuhmann[26],
B. Schwab[14], A. Schwind[35], F. Sefkow[11], M. Seidel[12], R. Sell[11], A. Semenov[23], V. Shekelyan[11],
I. Sheviakov[24], H. Shooshtari[26], L.N. Shtarkov[24], G. Siegmon[16], U. Siewert[16], Y. Sirois[28],
I.O. Skillicorn[10], P. Smirnov[24], J.R. Smith[7], V. Solochenko[23], Y. Soloviev[24], J. Spiekermann[8],
S. Spielman[28], H. Spitzer[13], R. Starosta[1], M. Steenbock[13], P. Steffen[11], R. Steinberg[2], B. Stella[32],
K. Stephens[22], J. Stier[11], J. Stiewe[15], U. Stösslein[35], K. Stolze[35], J. Strachota[30], U. Straumann[37],
W. Struczinski[2], J.P. Sutton[3], S. Tapprogge[15], V. Tchernyshov[23], C. Thiebaux[28], G. Thompson[20],
P. Truöl[37], J. Turnau[6], J. Tutas[14], P. Uelkes[2], A. Usik[24], S. Valkár[31], A. Valkárová[31], C. Vallée[25],
P. Van Esch[4], P. Van Mechelen[4], A. Vartapetian[11,38], Y. Vazdik[24], P. Verrecchia[9], G. Villet[9],
K. Wacker[8], A. Wagener[2], M. Wagener[33], I.W. Walker[18], A. Walther[8], G. Weber[13], M. Weber[11],
D. Wegener[8], A. Wegner[11], H.P. Wellisch[26], L.R. West[3], S. Willard[7], M. Winde[35], G.-G. Winter[11],
C. Wittek[13], A.E. Wright[22], E. Wünsch[11], N. Wulff[11], T.P. Yiou[29], J. Žáček[31], D. Zarbock[12],
Z. Zhang[27], A. Zhokin[23], M. Zimmer[11], W. Zimmermann[11], F. Zomer[27], and K. Zuber[15]

[1] I. Physikalisches Institut der RWTH, Aachen, Germany[a]
[2] III. Physikalisches Institut der RWTH, Aachen, Germany[a]
[3] School of Physics and Space Research, University of Birmingham, Birmingham, UK[b]
[4] Inter-University Institute for High Energies ULB-VUB, Brussels; Universitaire Instelling Antwerpen, Wilrijk, Belgium[c]
[5] Rutherford Appleton Laboratory, Chilton, Didcot, UK[b]
[6] Institute for Nuclear Physics, Cracow, Poland[d]
[7] Physics Department and IIRPA, University of California, Davis, California, USA[e]
[8] Institut für Physik, Universität Dortmund, Dortmund, Germany[a]
[9] CEA, DSM/DAPNIA, CE-Saclay, Gif-sur-Yvette, France
[10] Department of Physics and Astronomy, University of Glasgow, Glasgow, UK[b]
[11] DESY, Hamburg, Germany[a]
[12] I. Institut für Experimentalphysik, Universität Hamburg, Hamburg, Germany[a]
[13] II. Institut für Experimentalphysik, Universität Hamburg, Hamburg, Germany[a]
[14] Physikalisches Institut, Universität Heidelberg, Heidelberg, Germany[a]
[15] Institut für Hochenergiephysik, Universität Heidelberg, Heidelberg, Germany[a]
[16] Institut für Reine und Angewandte Kernphysik, Universität Kiel, Kiel, Germany[a]
[17] Institute of Experimental Physics, Slovak Academy of Sciences, Košice, Slovak Republic[f]
[18] School of Physics and Materials, University of Lancaster, Lancaster, UK[b]
[19] Department of Physics, University of Liverpool, Liverpool, UK[b]
[20] Queen Mary and Westfield College, London, UK[b]
[21] Physics Department, University of Lund, Lund, Sweden[g]
[22] Physics Department, University of Manchester, Manchester, UK[b]
[23] Institute for Theoretical and Experimental Physics, Moscow, Russia
[24] Lebedev Physical Institute, Moscow, Russia[f]
[25] CPPM, Université d'Aix-Marseille II, IN2P3-CNRS, Marseille, France
[26] Max-Planck-Institut für Physik, München, Germany[a]
[27] LAL, Université de Paris-Sud, IN2P3-CNRS, Orsay, France
[28] LPNHE, Ecole Polytechnique, IN2P3-CNRS, Palaiseau, France
[29] LPNHE, Universités Paris VI and VII, IN2P3-CNRS, Paris, France

[30] Institute of Physics, Czech Academy of Sciences, Praha, Czech Republic[f,h]
[31] Nuclear Center, Charles University, Praha, Czech Republic[f,h]
[32] INFN Roma and Dipartimento di Fisica, Universita "La Sapienza", Roma, Italy
[33] Paul Scherrer Institut, Villigen, Switzerland
[34] Fachbereich Physik, Bergische Universität Gesamthochschule Wuppertal, Wuppertal, Germany[a]
[35] DESY, Institut für Hochenergiephysik, Zeuthen, Germany[a]
[36] Institut für Teilchenphysik, ETH, Zürich, Switzerland[i]
[37] Physik-Institut der Universität Zürich, Zürich, Switzerland[i]
[38] Visitor from Yerevan Phys.Inst., Armenia

[a] Supported by the Bundesministerium für Forschung und Technologie, FRG under contract numbers 6AC17P, 6AC47P, 6DO57I, 6HH17P, 6HH27I, 6HD17I, 6HD27I, 6KI17P, 6MP17I, and 6WT87P
[b] Supported by the UK Particle Physics and Astronomy Research Council, and formerly by the UK Science and Engineering Research Council
[c] Supported by FNRS-NFWO, IISN-IIKW
[d] Supported by the Polish State Committee for Scientific Research, grant No. 204209101
[e] Supported in part by USDOE grant DE F603 91ER40674
[f] Supported by the Deutsche Forschungsgemeinschaft
[g] Supported by the Swedish Natural Science Research Council
[h] Supported by GA ČR, grant no. 202/93/2423 and by GA AV ČR, grant no. 19095
[i] Supported by the Swiss National Science Foundation

1. Introduction

This paper analyses the spectra of hadrons produced in deep inelastic scattering (DIS) e^-p collisions as a function of both the four-momentum squared ($q^2 = -Q^2$) transferred from the electron and the Bjorken scaling variable, x. In terms of the proton four momentum P, x is defined as $Q^2/2P \cdot q$, but it may be naïvely thought of as the momentum fraction of the struck quark in the proton. We also select on the basis of the dimensionless inelasticity variable $y = Q^2/xs$ where $\sqrt{s}$ is the overall e^-p centre of mass energy. The H1 collaboration has already published charged particle spectra, analysed in the hadronic centre of mass (CMS) frame, in intervals of the total hadronic mass, W (where $W^2 \approx Q^2(1/x - 1)$), using 22.5 nb^{-1} of data obtained in the first year of HERA operation [1]. It is the aim of the present analysis to use the increased statistics of 1993 data to cast such spectra into the form of fragmentation functions which are reliably related to the hadronisation of quarks. Aspects of these distributions can then be used in a comparison with corresponding data from e^+e^- experiments [2] to determine the relevant evolution variable for such distributions.

Since the initial state of e^+e^- annihilation interactions is a neutral off mass-shell photon or Z^0, all events with only hadrons in the final state are the result of a pure quark-antiquark pair creation process. Hard interactions in pp or $p\bar{p}$ collisions are much more complicated. Apart from the effect of the proton-remnant hadronisation, initial state QCD radiation predominantly involving gluons is important. In addition gluon-gluon interactions dominate the hard scatter. Quark identification can only be performed statistically and in very limited kinematic areas. In e^-p interactions at HERA there are fewer problems caused by the proton remnant

and, to first order, the virtual photon couples only to charged quarks. Electron kinematics alone can give the final state quark kinematics thus enabling a study of its hadronic fragments for direct comparison with quark fragmentation in e^+e^- interactions.

The momentum distribution of the hadrons from quark fragmentation in e^+e^- interactions roughly scales with $\sqrt{s_{ee}} = E^*$, the overall centre of mass system (CMS) energy. The ratio of the momentum of a given charged hadron to the maximum energy that it could have, $x_p = 2p^{\pm}_{hadron}/E^*$, is thus a natural variable in terms of which e^+e^- experiments [2,3] have described hadronic spectra. It has the advantage of being independent of the difficulties involved in any jet or thrust axis determination. The variable is manifestly not Lorentz invariant and it will therefore become necessary to identify an equivalent frame for e^-p interactions in which comparisons can properly be made.

The distribution $D^{\pm}(x_p) = (1/N_{evts}) \times dn^{\pm}_{tracks}/dx_p$, being a charged track density normalised by the number of events, is termed the fragmentation function. It characterises the complete process which includes parton shower development as well as non-perturbative hadronisation. In principle the fragmentation function is unique only to a given quark and hadron species, but tagging techniques usually dictate that the data is effectively an integrated average. It is a "soft" function rising rapidly as x_p decreases but then turning over near $x_p = 0$. A related distribution is that of the arbitrarily normalised logarithm of track energies where the turn-over becomes the "hump-backed" plateau [4].

The variable $\xi = \ln(1/x_p)$ expands the turn-over region, and the expectation of the Modified Leading Logarithmic Approximation (MLLA) to perturbative QCD predicts that for partons ξ is distributed in a roughly Gaussian manner. Assuming Local Parton-Hadron Duality (LPHD) the same behaviour is expected for any type of hadron with the mean ξ increasing as $\ln(E^*)$ and the area under the Gaussian (multiplicity) increasing only slightly faster [5]. More detailed expectations of the fragmentation stem from the influence of quantum-mechanical coherence between gluons in the time-like parton shower [6]. Effectively this reduces the available phase space for soft gluon emission to an angular ordered region. This coherence should then reduce the gradient of the energy dependence of the peak position.

In e^-p interactions there is no exact equivalent of the e^+e^- centre of mass system. The hadronic (γp) CMS is one candidate. In the naïve quark parton model (QPM) the final state then contains a quark which is back to back with the spectator system. This collaboration has already published [1] $x_F = p_z/p_{max}$ distributions in this frame for the hemisphere opposite to the direction of travel of the incoming proton and outgoing remnant.

A further boost along the z-(virtual photon)axis gives the Breit frame defined in this analysis such that the positive z-direction is that of the incoming quark and the negative direction that of the incoming photon. This frame is defined such that the virtual photon is entirely space-like, having a momentum of $p_z = -Q$. Within the QPM a quark has momentum $p_z = +Q/2$ before and $p_z = -Q/2$ after scattering and therefore, in this frame, $x_p = 2p^{\pm}_{hadron}/Q$ is the equivalent of the e^+e^- definition of a fragmentation variable[1]. QCD radiation alters these values and implies that the collision is no longer collinear. In particular

[1]Note that since Q^2 is defined as a positive quantity one can refer to a value of 'Q' for the event. References [7] discuss other possible variables in the Breit frame incorporating, for example, $p_{\parallel}$ which gives directional information. Since the main aim of this paper is to compare with e^+e^- experiments, we have chosen to remain with a compatible definition.

initial-state radiation of gluons has no equivalent in an e^+e^- event. Note that whereas a given e^+e^- experiment has one fixed value of E^*, an e^-p experiment results in a wide range of Q enabling evolution of the fragmentation function to be tested in a single experiment. Conversely the fragmentation function should now be considered to be the result of a convolution with the structure functions of the individual quarks. This analysis will ignore this effect but will look for variations of fragmentation as a function of the event x as well as Q^2.

The Breit frame is defined solely by the kinematics of the virtual current and is concerned more with the quark-current rather than the proton-current interaction. The spectator system has reduced significance. Thus, despite some difficulties [8], the negative z hemisphere of this frame, rather than the γp CMS, has been suggested [5] as a better approximation to one half of the e^+e^- CMS. Monte Carlo comparisons have been made [9,10] to indicate the possibility of making the kind of measurements presented here. These analyses merely *define* a given hemisphere to contain current or target-associated tracks but in this analysis we shall also make some attempt to assess the confidence with which such associations may be made. Quantum-mechanically there is no absolute meaning for such associations, but as with the existence of jets, there are useful approximations which can be made. Since the γp CMS and the Breit frames are linked by a boost, they cannot in general both have the same negative z hemisphere content so the question of relative loss and contamination is worthy of empirical examination.

2. The H1 Experiment

This analysis uses data from 1993 when the HERA e^-p collider was run with a proton beam of 820 GeV and an electron beam of 26.7 GeV. A detailed description of the H1-detector has been given elsewhere [11]. This paper will thus give only a short description of components vital for this analysis.

Momentum measurements of charged tracks are provided, in the central region, by two cylindrical and co-axial drift chambers [12] for (r, ϕ) measurement supplemented by two z-chambers; in the forward (proton) direction they are provided by three Radial and three Planar drift chamber modules [13]. These track detectors are inside a uniform 1.15 T magnetic field. Track segments from all devices are combined to give efficient detection and momentum measurement with $\delta p/p^2$ better than 1% /GeV in the angular range used in this analysis, $10^\circ < \theta < 160^\circ$. A full Monte Carlo simulation based on GEANT [14] gives an acceptable description of the effect of dead areas and reconstruction efficiency.

In the polar angle range $4^\circ < \theta < 153^\circ$ the trackers are surrounded by a fine-grained liquid argon (LAr) sampling calorimeter [15] with lead and steel absorbers in the electromagnetic and hadronic sections, respectively. The calorimeter cells measure hadronic energy flow and the energy of the scattered electron for high Q^2 events. The LAr calorimeter is complemented by a backward electromagnetic, lead-scintillator, calorimeter (BEMC) covering the angular range $151^\circ < \theta < 176^\circ$. The data are divided into two separate samples for low and high Q^2 where the scattered electron energy is well contained in either but not both of the two calorimeters. There are possible systematic energy scale errors taken to be $\pm 1.7\%$ for the BEMC and $\pm 3\%$ for the LAr calorimeter.

Data Sample	Non diffractive events	Good central calorimetry	Breit frame energy flow
$12 < Q^2 < 80$ GeV^2	5927	3141	1945
$Q^2 > 100$ GeV^2	423	373	235

Table 1: *Size of data samples for this analysis. See text for definition of selections.*

3. Data Selection and Acceptance Corrections

The source data for this analysis come from the late period of 1993 when magnetic field was reestablished in the H1 detector. Selections to further limit data only to periods when there were extremely stable tracking conditions and when there was no coincident problem with electronic 'noise' in the H1 calorimetry give a total integrated luminosity for this subset of ≈ 150 nb^{-1}.

A neutral current DIS event selection is made by demanding a well-reconstructed scattered electron of energy greater than 14 GeV. The selection $12 < Q^2 < 80$ GeV^2 defines the BEMC sample, whereas the requirement for the scattered electron to have a polar angle in the range $10^\circ < \theta < 150^\circ$ (resulting in the constraint $Q^2 > 100$ GeV^2) defines the LAr sample. These data sets are referred to as the low and high Q^2 samples, respectively. In terms of the usual DIS variables further cuts of $W^2 > 3000$ GeV^2 and, in the case of high Q^2, $y < 0.6$ are applied to maintain high acceptance, and to avoid radiative corrections and contamination from photoproduction events. The final sample is better than 99.7% pure DIS. Additional cuts [1] are made to exclude possible diffractive events (about 6% of the sample) where the virtual photon may be said to interact with a Pomeron-like object [16]. There is no equivalent in the e^+e^- interactions with which we intend to compare and such events are not adequately described by our DIS Monte Carlo generators with which we perform acceptance corrections. In practice this removal is done by demanding that there is at least 0.5 GeV deposit of observable energy in the polar region $4.4^\circ < \theta < 15^\circ$. The resultant event numbers are given as the first column in Table 1.

Within these events, charged tracks are selected with $\delta p/p < 1$ and with transverse momentum $p_t > 150$ MeV/c in the central tracker or momentum $p > 500$ MeV/c in the forward tracker. The tracks are also required to satisfy basic quality criteria on total number of digitisations, quality of vertex fits etc. Together these selections give a smooth variation in acceptance over the whole angular range. Cuts are made to remove tracks not originating from the primary interaction vertex but these fail to exclude roughly half of the $\approx 4\%$ of tracks arising from K^0_s decays.

Corrections for the effect of all of these cuts, and for the contribution of remaining K^0 and Λ decay products, are made by reconstructing Monte Carlo events with the same code and selections and then comparing these with results for primary charged particles at the generated event level. Commonly, LEPTO 6.1 [1] is used with MRS H structure functions and with a Colour Dipole model [17] for gluon radiation, but a version with matrix elements matched to parton showers in the MLLA approximation [18] has also been used and we note no significant change in any of the results. Since corrections are made bin-by-bin, in narrow

kinematic areas, and with *ratios* of generated to reconstructed track numbers the analysis is rather insensitive to Monte Carlo physics assumptions.

4. Breit Frame Event Selection

It is the aim of this analysis to select well-measured events requiring small acceptance corrections for analysis of tracks in the Breit frame of reference. This may be done using calorimetery information alone in order to avoid track reconstruction bias. First four-momentum vectors which correspond to the direction and energy of calorimeter clusters (assuming pion masses) are boosted to the Breit frame using the (x, Q^2) values calculated solely from the electron kinematics. The $z < 0$ hemisphere, commonly referred to as the current fragmentation region, is then examined in more detail. To ensure that events have good and uniform track acceptance a selection is made such that events are taken for further analysis if 95% or more of the observed energy in this hemisphere originates from the laboratory polar region $10° < \theta < 150°$. This region is completely covered by the (LAr) calorimetry and thus has consistent calibration. The numbers of such events surviving this cut are also given in Table 1 in the column headed 'good central calorimetry'.

For each event, the four-momenta of all energy clusters in the $z < 0$ hemisphere are added and the resultant total energy $E_{z<0}$, is plotted as a fraction of the event Q against the resultant cosine of the Breit frame polar angle, $\cos\Theta_{BF}$, in Fig. 1. According to the QPM, a quark would be expected to have energy $Q/2$ and $\cos\Theta_{BF} = -1$. At high Q^2 there is a tendency for the events to cluster in the area of this point. However, the spread of events is much greater at low Q^2 and there are a large number of events with small energy in the 'current' hemisphere and/or with a net cluster emerging at a large angle with respect to the beam axis. If, for a given event, the net energy flow is only just within the current hemisphere there could be some risk of bias in measuring the share of that energy. Simulated events samples behave in exactly the same way as the data and studies have shown that this spread is mainly because of reconstruction effects. Simple rejection of such events is a little problematic however as, at the generated level, some of these events show slightly different properties because of the loss of tracks to the target hemisphere through significant QCD radiation some of which would also have its equivalent in e^+e^- interactions. We thus choose to test the possibilities of bias by performing the analysis both on all events and also by rejecting events below the line joining $E_{z<0} = 0$, $\cos\Theta_{BF} = -1$ to $E_{z<0} = Q/2$, $\cos\Theta_{BF} = 0$ indicated in Fig. 1 and referred to as the Breit frame energy flow selection. The event numbers surviving this topological selection are given as the final column in Table 1.

Having selected events using calorimetry, *track* properties in the Breit frame are now investigated, beginning with the distribution of $\cos\theta_B$, the cosine of the polar angle for charged particles, as shown in Fig. 2(a,b).

These data have bin-by-bin corrections for losses due to acceptance and inefficiencies calculated using simulated and reconstructed Monte Carlo events. For $-1 < \cos\theta_B < 0.99$, avoiding effects in this frame due to the beam pipe, the average correction factor is 1.35 for the low Q^2 sample and 1.42 for the high Q^2 sample. The correction factors are small and vary smoothly for $\cos\theta < 0.0$. There is an obvious peak in the positive-z (beam) direction and also in the negative-z (quark) direction at high Q^2 but which is much less clear at low momentum transfer.

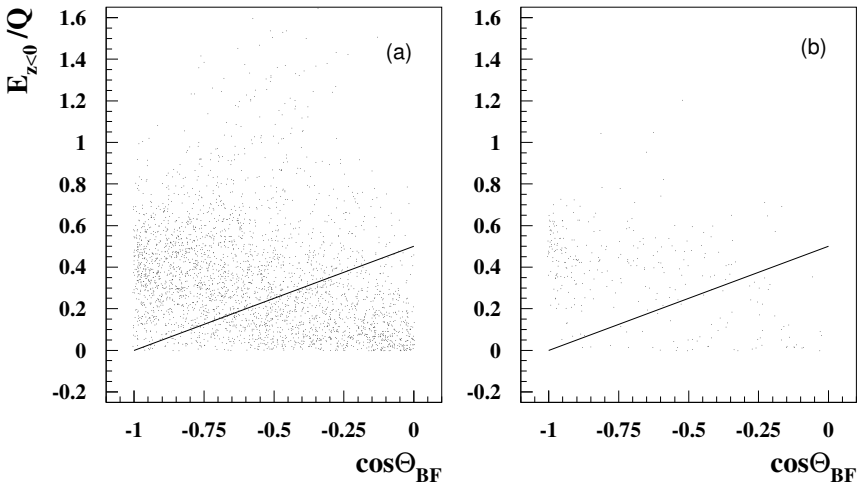

Figure 1: *The total energy of the summed calorimeter cluster four momentum vectors in the $z < 0$ hemisphere of the Breit frame is plotted as a fraction of the event Q against the cosine of the polar angle of the resultant vector, for (a) the low Q^2 and (b) the high Q^2 sample. The line indicates the cut for the secondary analysis described in the text.*

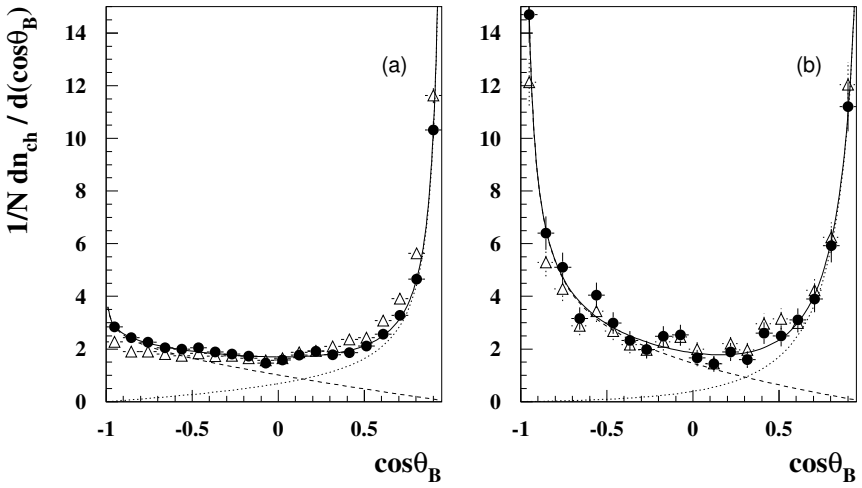

Figure 2: *Distribution of the cosine of the Breit frame polar angle for tracks of (a) the low Q^2 and (b) the high Q^2 sample, with statistical errors only. The open triangles show the data before the Breit frame energy flow selection. The solid line corresponds to the empirical fit described in the text, where the dashed line is the nominal quark contribution and the dotted line that of the target.*

In strict quantum-mechanical interpretation, no track can be said to 'belong' to either the jet or target remnant, wherever it lies in the Breit frame. It is clear from Fig. 2 however that the concept of current and target hemispheres is a good approximation as Q^2 increases but almost a question of mere definition at our lowest Q^2 values. We adopt two different procedures to estimate the possible loss or contamination involved in using a selection of one hemisphere of the Breit frame to represent the quark behaviour. In Fig. 2 there are empirical fits to $Ae^{-a(1+x)^\alpha}(1-x)+Be^{-b(1-x)^\beta}(1+x)$, where $x=\cos\theta_B$. This and fits to other possible functional forms suggest that, in the Breit frame, the selection $\cos\theta_B < 0.0$ roughly equalises loss and contamination between the current and target fragmentation and that they are at the $< 5\%$ level at high Q^2 but at the $\approx 20-25\%$ level at low Q^2. Our method of correction by Monte Carlo simulation accounts for migration between hemispheres caused by resolution effects. A separate study showed that these are dominated by measurement errors of the reconstructed electron giving an incorrect boost rather than track measurement errors. The magnitude of migration losses and contaminations are commensurate with the various empirical fits suggesting that these latter are indeed dominated by poor reconstruction. It is the approach of this analysis to adopt $\cos\theta_B < 0.0$ as our selection for tracks. If it is further required to associate these particle multiplicities with a quark we feel that an additional $20(5)\%$ systematic error on the particle multiplicity of low(high) Q^2 data should be imposed to describe our remaining ignorance of current/target separation.

5. Fragmentation Functions

The charged particle fragmentation functions, as defined in the introduction, are displayed in Fig. 3(a,b) as a function of $x_p = 2p^{\pm}_{hadron}/Q$ for the current hemisphere of the Breit frame and for the two Q^2 intervals. These figures utilise the selections of the previous section including the Breit frame energy flow selection. The individual fragmentation functions, for positive and negative hadrons, are indistinguishable, at least with the present statistics in the current kinematic areas of investigation, and are treated inclusively for the rest of this paper. Changing the fragmentation variable to be $\xi = \ln(1/x_p)$ and defining the fragmentation function to be $D(\xi) = (1/N_{evts}) \times dn_{tracks}/d\xi$ results in the Gaussian shape of Fig. 4(a,b) expected from the discussion in section 1 and seen also in e^+e^- data. The area increases and the peak moves to higher values of ξ at higher Q^2. These distributions are also corrected bin-by-bin for acceptance and efficiency, although again the dependence is smooth and small[2] especially in the case of the variable ξ. Simulation studies show that the resolution in ξ ($\delta\xi \approx 0.12$), again dominated by the uncertainties in the boost to the Breit frame is smaller than the bin-width of 0.2 in ξ used throughout in this analysis.

The low and high Q^2 data of Fig. 4 have each been further subdivided to give a total of ten intervals of Q in order to study the evolution of the area, peak and width of the fragmentation function in more detail. The variation of the integrated area (equal to the mean charged particle multiplicity, $< n_{ch} >$) is shown in Fig. 5 and the results are reproduced in Table 2. The systematic errors described at the end of section 4 dominate but are added in quadrature with statistical errors. The figure and table show the results obtained both with and without the Breit frame energy flow selections described in section 4 since there appears

[2]The effect of remaining QED radiative corrections to the Born term has been investigated using the Monte Carlo program Django 2.1 [19]. This analysis shows no effective variation over the peak area but an overall normalisation correction of $+4.3\pm0.3\%$ has been included within our corrections, although it is small compared with other sources of error.

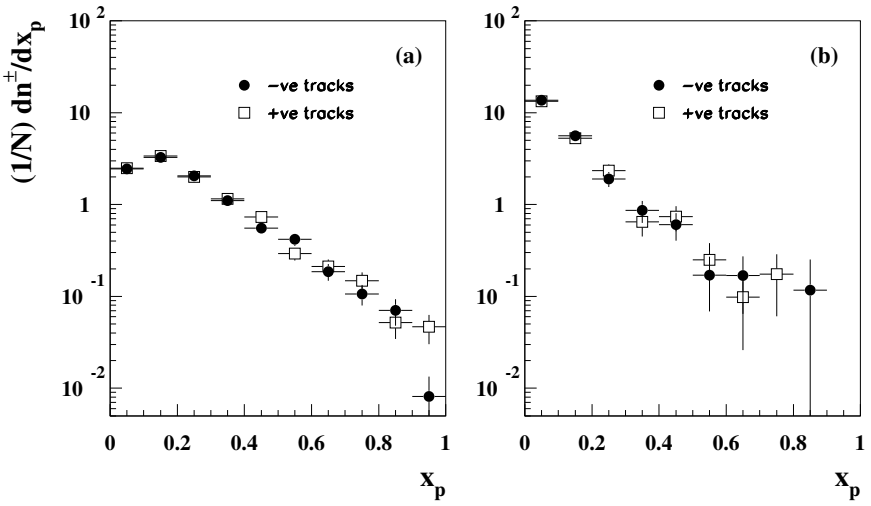

Figure 3: *The fragmentation functions, $D^{\pm}(x_p)$, for the current hemisphere of the Breit frame shown separately for positive and negative tracks, for (a) the low Q^2 and (b) the high Q^2 sample with statistical errors only.*

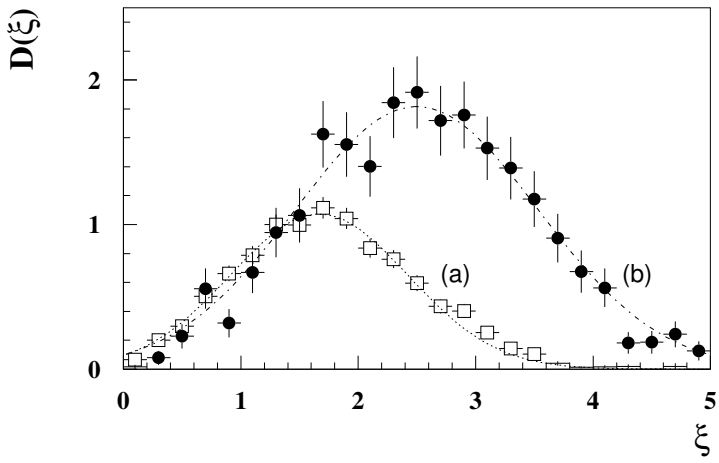

Figure 4: *The fragmentation functions for the current hemisphere of the Breit frame, $D(\xi)$, for (a) the low Q^2 and (b) the high Q^2 sample, with statistical errors only and with simple Gaussian fits superimposed.*

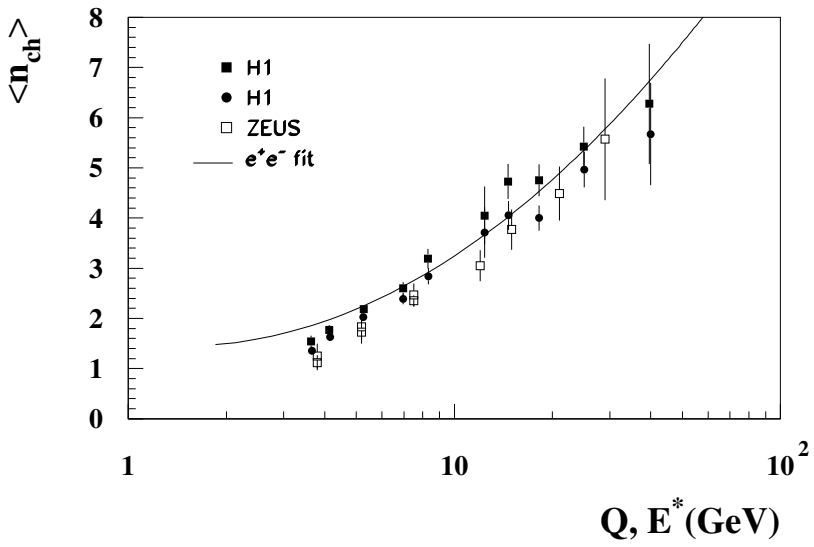

Figure 5: *Average charged particle multiplicity in the current region of the Breit frame for data before (solid circles) and after (solid squares) the energy flow selection as a function of Q compared with a parameterisation (line) of one half of average corrected track multiplicities in e^+e^- events as a function of E^*. The results of a ZEUS analysis are shown as open squares, with points at the same Q being at different x.*

to be a significant difference, especially at low Q^2. Since these data are corrected for known acceptance effects we ascribe this difference to QCD radiation depositing particles in the target hemisphere. It is seen similarly at the generated level of Monte Carlo. The difference is indicative of difficulties of detail inherent in a comparison with e^+e^- data. A fit [20] to many e^+e^- data points[3] is also shown for comparison as a function of E^*. At low Q our results, and those of the ZEUS experiment [21], comparable to the H1 results with no selection, show a significantly lower average charged multiplicity but compatible with differences that might be expected from differing QCD radiation effects.

At a detailed level, agreement between particle multiplicities can also not be expected to be precise because of the comparative 'flavour democracy' expected in e^+e^- annihilation. Jets initiated by b-quarks, constituting some 22% of e^+e^- events, have roughly 13% higher average charged multiplicity at LEP energies [22]. Such flavour effects are thus at the 3% level which is much less significant than our present errors and we make no attempt to correct for them. There is no doubt from this figure that Q is a suitable scaling quantity equivalent to E^* in e^+e^- interactions. Low energy, fixed target data [23] indicated agreement between average

[3]Note that the published results refer to e^+e^- *events*. Average track multiplicities have been reduced by a factor two to correspond to results for each *quark* and a further 8.1% (the average of available data) reduction has been made to account for K^0 and Λ decay tracks.

Q^2 Interval	Energy Flow Selection			Total Current Hemisphere		
(GeV^2)	Multiplicity	Peak	Width	Multiplicity	Peak	Width
12 → 15	1.54±0.11	1.41±0.13	0.83±0.14	1.35±0.08	1.45±0.08	0.72±0.08
15 → 20	1.77±0.10	1.47±0.10	0.72±0.07	1.63±0.08	1.49±0.08	0.82±0.09
20 → 40	2.18±0.08	1.63±0.09	0.71±0.04	2.02±0.06	1.66±0.06	0.74±0.04
40 → 60	2.60±0.13	1.91±0.11	0.83±0.10	2.39±0.11	1.94±0.09	0.91±0.11
60 → 80	3.20±0.19	2.00±0.12	0.83±0.12	2.84±0.16	2.01±0.10	0.87±0.13
100 → 175	4.05±0.58	2.23±0.39	1.00±0.71	3.71±0.50	2.27±0.17	0.75±0.27
175 → 250	4.73±0.35	2.12±0.34	1.28±0.50	4.05±0.29	2.18±0.30	1.26±0.48
250 → 450	4.75±0.32	2.72±0.29	1.24±0.45	4.00±0.25	2.68±0.23	1.09±0.32
450 → 1000	5.43±0.39	2.70±0.13	0.80±0.15	4.97±0.36	2.71±0.16	0.79±0.17
1000 → 8000	6.27±1.20	2.62±0.28	0.88±0.39	5.67±1.02	2.63±0.26	0.85±0.35

Table 2: *Average charged particle multiplicity, peak and width of the fragmentation function for the Q^2 intervals given using either the energy flow selection or the total current hemisphere of the Breit frame.*

charged particle multiplicities in the current hemisphere of the hadronic CMS frame and those of e^+e^- with E^* at the same W but later experiments [1,24] show significant disagreements at low Feynman-x. These analyses do not, in any case, attempt to demonstrate the relatively clear current-target separation seen, at least at high Q^2, in this analysis.

The peak and width (σ) values of the fragmentation function may be found from Gaussian fits to the central area ($\pm$ one unit of ξ either side of the statistical mean) so as simultaneously to test MLLA predictions and to minimise dependence on Monte Carlo corrections which mainly affect the tails of the distributions. The simulated event studies referred to at the end of section 4 show that the resolution of a particle's polar angle in the Breit frame is much poorer than its momentum and indicate that at $\cos\theta_B \approx 0$, $\delta(\cos\theta_B) \approx \pm\ 0.40(0.25)$ at low(high) Q^2. This quantity does not enter into ξ but affects peak and width measurements through uncertainty in the selection of the negative Breit frame hemisphere. As an estimator of the systematic error that might be introduced because of this selection we have repeated the above analyses using the cuts at the $\pm$ one sigma level of these resolutions and use extreme differences of results as an estimate of systematic errors. For the peak values, this estimate gives a result which is, in general, of the order of the statistical fitting errors. There is an additional source of systematic error of $\approx \pm 6\%$ in ξ_{peak} which arises from uncertainty in the boost due to the calorimeter energy scale errors given at the end of section 2. These errors dominate all other sources of systematic error coming, for example, from using different Monte Carlo generators for corrections. Width measurements are completely dominated by statistical errors.

The results of these fits for both ξ_{peak} and ξ_{width} variation as a function of Q are given in Table 2 and are shown in Fig. 6(a,b), with all sources of error added in quadrature. The figure shows the results using our Breit frame energy flow selection but, as the results in the table indicate, there is only the suggestion of the peak values being slightly lower with the selection

rather than without. We may conclude that, within our errors, the parameters of this analysis are insensitive to the spectrum of hadronic fragments in QCD radiation lost to the target region and we therefore should still be able to compare with data from e^+e^- interactions. The published e^+e^- fragmentation function results [2,3] have been fitted using the same procedure and are shown at the appropriate e^+e^- E^* values. Clear agreement is again evident using Q as the appropriate equivalent variable. The peak values are also in agreement with those of the ZEUS analysis [21] where no selection within the current hemisphere was made.

If Q is taken to be equivalent to $\sqrt{s_{ee}}$ and is normalised by an effective energy scale to give a variable $Y = \ln(Q/2\Lambda_{\mathit{eff}})$ then, assuming gluon coherence, the predicted MLLA behaviour of the peak position and width is [5]

$$\xi_{peak} = 0.5Y + c_2\sqrt{Y} + O(1)$$

$$\xi_{width} = \sqrt{Y^{\frac{3}{2}}/2c_1}$$

where c_1, c_2 are constants dependent only on the number of colours and flavours in QCD, Λ_{eff} sets the scale of the mass of the final state fragmented hadrons, and $O(1)$ contains higher order corrections. Following [2] in assuming three flavours, we obtain $\Lambda_{\mathit{eff}} = 0.24 \pm 0.04$ GeV and $O(1) = -0.38 \pm 0.11$[4] in a combined fit (solid line) to the present peak and width data. These results are to be compared with the analysis [2] of e^+e^- ξ_{peak} evolution [2,3,25,26] which gives $\Lambda_{\mathit{eff}} = 0.21 \pm 0.02$ GeV and $O(1) = -0.32 \pm 0.06$. The dashed line of Fig. 6 shows the prediction at the generator level of the LEPTO 6.1 Monte Carlo with an assumption of gluon coherence in parton showers and using a Lund string model [27] for final hadronisation.

A straight line fit to ξ_{peak} as a function of $\ln(Q)$ gives a gradient of 0.75 ± 0.05. Reference [2] claims a significant need for gluon coherence, noting that a gradient of unity would be the naïve expectation if the multiplicity in a parton shower increased solely due to the constraints of longitudinal phase space. We find that abandoning the angular-ordering model of gluon coherence in the parton shower, but maintaining string hadronisation (dashed-dotted line in Fig. 6) gives almost indistinguishable evolution predictions. The results from HERWIG [28] (not shown) with cluster hadronisation are similarly indistinguishable. A crude implementation [29] of an independent fragmentation model with or without (dotted line) gluon coherence gives effective gradients only slightly below unity (0.94 ± 0.01 in this case, with our selections). However, we are aware of other implementations [30,31] which impose energy conservation on hadronic distributions of transverse momentum that reproduce the same kind of 'string' effects. We should conclude that the common e^-p /e^+e^- result does not constitute proof of the need for gluon coherence, and that the success of the MLLA-inspired model, even down to our lowest Q values, may be supporting claims [32] that the more fundamental cause of lower gradients is the increase of transverse momentum with energy.

There is an expected effect on the peak position due to the limited opening angle of the jet implied by the selection of the current hemisphere in the Breit frame [5]. This systematically rejects lower x_p, and hence higher ξ, tracks but there is a simultaneous inclusion of soft track contamination from the target. As we have shown, using one hemisphere of the Breit frame

[4]The evolution of the peak with Y is so nearly linear that there is a large correlation between the two parameters. This is resolved in our analysis by the width evolution which has no dependence on the $O(1)$ term.

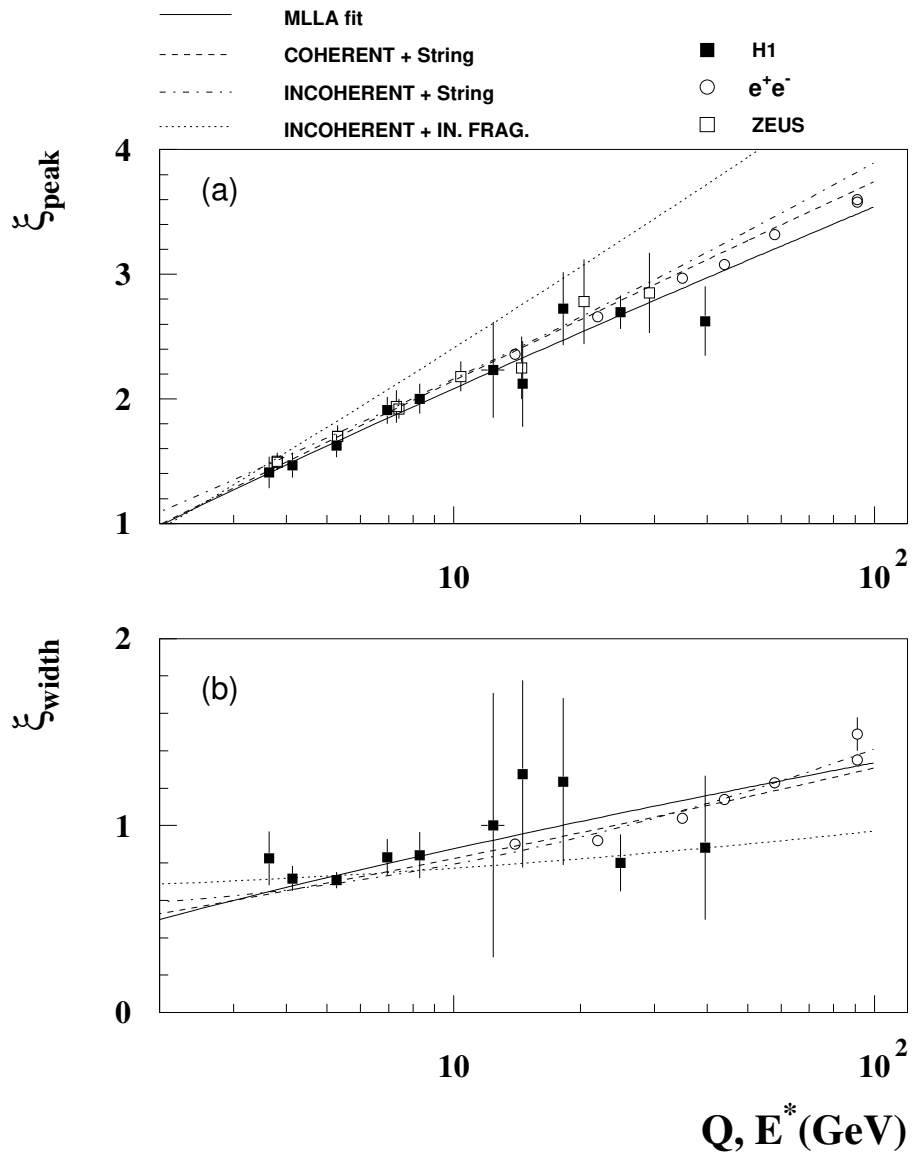

Figure 6: *Evolution of (a) the peak position and b) the width (σ) of a fitted Gaussian fragmentation function compared with similar fits to e^+e^- data and with the results of a ZEUS analysis, with points at the same Q being at different x. The solid line is a two-parameter simultaneous MLLA-expectation fit to the H1 data. See text for a discussion of the various model predictions.*

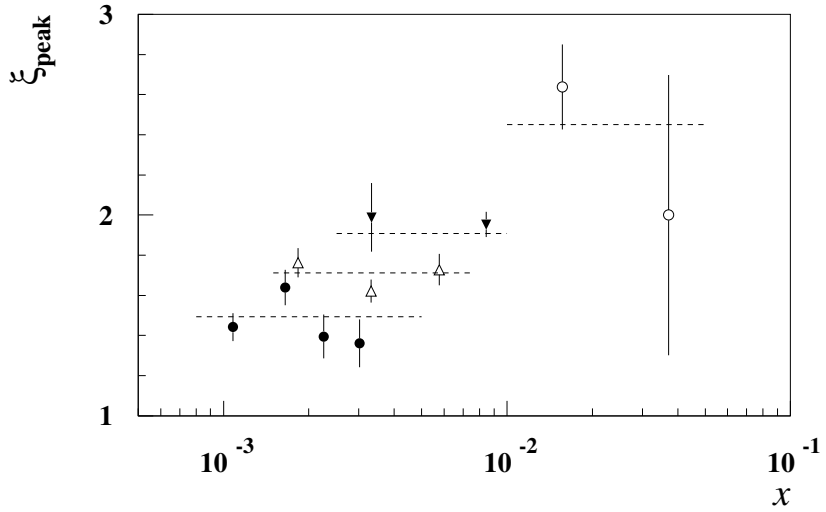

Figure 7: *Position of the fragmentation function peak as a function of Bjorken x, in the intervals (solid circles)* $12 < Q^2 < 25$ GeV^2*, (open triangles)* $25 < Q^2 < 45$ GeV^2*, (solid triangles)* $45 < Q^2 < 80$ GeV^2*, and (open circles)* $200 < Q^2 < 500$ GeV^2*. The dashed lines refer to the* ξ_{peak} *expected from the fit at the relevant mean* Q^2 *value.*

roughly equalises these effects but the investigations [33] of systematic errors which used cuts at the positions $\cos\theta_B = \pm 0.40, \pm 0.25$ as described earlier in this section show some evidence for a small systematic shift in the expected direction. The net effect is small and presently inconclusive.

6. Dependence on x

High Q^2 events are only accessible at high Bjorken x and this correlation is amplified by the W^2 and y cuts made in this analysis. Thus it is possible that the results presented so far are a reflected effect of a jet fragmentation evolution in terms of the parton momentum fraction x rather than Q^2. The expectations of MLLA are that, although distributions in the target region should show some x dependence [10], the peak of ξ in the current region should depend only on Q^2. The possibility of such x dependence has been investigated, suffering the consequent loss of statistics, by defining a number of rectangular (x,Q^2) cells well within acceptance limits and somewhat broader in Q^2 than previously used. The corrected values of ξ_{peak} are displayed in Fig. 7 as a function of x at constant Q^2, with statistical errors only. The dashed lines refer to the expected values as interpolated from the fit to the function given in the previous section. It is clear that these data indicate no observable x dependence.

7. Conclusions

This paper has shown that, when examined in the Breit frame as a function of Q, the basic features of the fragmentation function of charged particles in e^-p interactions are close to those of quarks pair-created in e^+e^- interactions when examined in their CMS as a function of $\sqrt{s_{ee}}$. In short, to a good approximation quarks behave in the same way in both methods of production and Q is a suitable variable with which to describe the evolution of their fragmentation. On the contrary there is no evidence for any dependence on x. The data of this paper are consistent with the evidence from e^+e^- data [2] for the need to incorporate gluon coherence in the description of this fragmentation, but Monte Carlo models *not* making this assumption are also able to reproduce both sets of data quite well.

8. Acknowledgements

We are grateful to the HERA machine group whose outstanding efforts made this experiment possible. We thank the engineers and technicians for their work in constructing and now maintaining the H1 detector, our funding agencies for financial support, the DESY technical staff for continual assistance, and the DESY directorate for the hospitality they extend to the non-DESY members of the collaboration.

References

1. H1 Collaboration, I. Abt et al., Zeit. Phys. C63 (1994) 377; The appendix to this publication also describes the Monte Carlo generators used in this analysis.
2. OPAL Collaboration, M.Z. Akrawy et al., Phys. Lett. 247B (1990) 617.
3. TASSO Collaboration, W. Braunschweig et al., Zeit. Phys. C47 (1990) 187.
4. Yu.L. Dokshitzer, V.S. Fadin and V.A. Khoze, Phys. Lett. 115B (1982) 242,Zeit. Phys. C15 (1982) 325. A.H. Mueller, Nucl. Phys. 213B (1983) 85, Nucl. Phys. 241B (1984) 141.
5. Yu.L. Dokshitzer, V.A. Khoze, A.H. Mueller and S.I. Troyan, "Basics of Perturbative QCD" Editions Frontières (1991); Ya.I. Azimov, Yu.L. Dokshitzer, V.A. Khoze, and S.I. Troyan, Zeit. Phys. C31 (1986) 213, Zeit. Phys. C27 (1985) 65; L.V. Gribov, Yu.L. Dokshitzer, V.A. Khoze, and S.I. Troyan, Phys. Lett. 202B (1988) 276,
6. A.H.Mueller, Phys. Lett. 104B (1981) 161; A. Bassetto, M. Ciafaloni, G. Marchesini and A.H. Mueller, Nucl. Phys. 207B (1982) 189; B.I. Ermolaev and V.S. Fadin, JETP Lett.33 (1981) 269; Yu.L. Dokshitzer et al., Rev. Mod. Phys. 60 (1988) 373.
7. N. Sakai, Phys. Lett. 85B (1979) 67; J. Sheiman, Nucl. Phys. 171B (1980) 445; P. Allen et al., Nucl. Phys. 176B (1980) 333.
8. G. Thompson et al., J. Phys. G19 (1993) 1575.

9. K. Charchula, J. Phys. G19 (1993) 1587.

10. G. Ingelman and J. Rathsman, J. Phys. G19 (1993) 1594.

11. H1 Collaboration, I. Abt et al., DESY preprint 93-103 (1993), submitted to Nucl. Instr. Meth.

12. J. Bürger et al., Nucl. Instr. Meth. A279 (1989) 217.

13. H1 FTD group, S.Burke et al., submitted to Nucl. Instr. Meth.

14. R. Brun et al., GEANT3 User's Guide, CERN preprint CERN-DD/EE 84-1.(1987)

15. H1 calorimeter group, B. Andrieu et al., Nucl. Instr. Meth. A336 (1993) 460.

16. H1 Collaboration, I. Abt etal., Nucl. Phys. 429B (1994) 477.

17. L. Lönnblad, Computer Phys. Comm. 43 (1992) 367.

18. G. Ingelman, Proc. HERA workshop, W. Buchmüller, G. Ingelmann (eds.), Hamburg (1991) vol.3, 1366; H. Bentsson, G. Ingelmann, and T.J. Sjöstrand, Nucl. Phys. 301B (1988) 554.

19. G.A. Schuler and H. Spiesberger. Physics at HERA Workshop Vol.3, (1991) 1419.

20. OPAL collaboration, P.D. Acton et al., Zeit. Phys. C53 (1992) 539.

21. ZEUS Collaboration, DESY preprint DESY 95-007, 1995.

22. DELPHI Collaboration, P. Abreu et al., Phys. Lett. 347B (1995) 447.

23. EMC, M. Arneodo et al., Nucl. Phys. 258B (1985) 249.

24. EMC, M. Arneodo et al., Zeit. Phys. C35 (1987) 417; E665 Collaboration, Phys. Lett. 272B (1991) 163.

25. L3 Collaboration, B. Adeva et al., Phys. Lett. 259B (1991) 199.

26. TOPAZ Collaboration, R. Itoh et al., Phys. Lett. 345B (1995) 335.

27. B. Andersson, G. Gustafson, G. Ingelman and T. Sjöstrand, Phys. Rep. 97 (1983) 31; T. Sjöstrand, Nucl. Phys. 248B (1984) 469.

28. G. Marchesini et al., Computer Phys. Comm. 67 (1992) 465.

29. T.J. Sjöstrand, CERN preprint CERN-TH.7112/93 and Computer Phys. Comm. 43 (1987) 367.

30. P. Mazzanti and R. Odorico, Nucl. Phys. 370B (1992) 23.

31. P. Biddulph and G. Thompson, Computer Phys. Comm. 54 (1989) 13.

32. E.R. Boudinov, P.V. Chliapnikov and V.A. Uvarov, Phys. Lett. 309B (1993) 210.

33. D. Kant, University of London thesis, to be published.